


# "Basicles": Microbial Growth and Production Monitoring in Giant Lipid Vesicles

**Journal Article****Author(s):**

Jusková, Petra; Schmid, Yannick R.F.; Stucki, Ariane; Schmitt, Steven; Held, Martin; [Dittrich, Petra S.](#) 

**Publication date:**

2019-09-25

**Permanent link:**

<https://doi.org/10.3929/ethz-b-000370767>

**Rights / license:**

[In Copyright - Non-Commercial Use Permitted](#)

**Originally published in:**

ACS Applied Materials & Interfaces 11(38), <https://doi.org/10.1021/acsami.9b12169>

**Funding acknowledgement:**

167123 - Microfluidic device for ultrarapid phenotypic susceptibility testing of pathogenic microbes (SNF)

681587 - Engineering of hybrid cells using lab-on-chip technology (EC)

# “Basicles”: Microbial Growth and Production Monitoring in Giant Lipid Vesicles

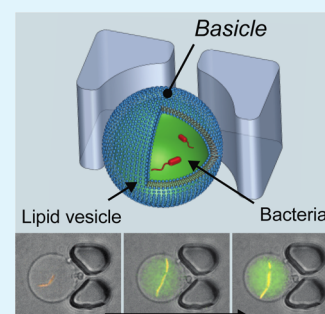
Petra Jusková,<sup>†,#</sup> Yannick R. F. Schmid,<sup>†,#</sup> Ariane Stucki,<sup>†</sup> Steven Schmitt,<sup>‡,§</sup> Martin Held,<sup>‡</sup> and Petra S. Dittrich<sup>\*,†,§</sup>

<sup>†</sup>Department of Biosystems Science and Engineering, Bioanalytics Group, and <sup>‡</sup>Department of Biosystems Science and Engineering, Bioprocess Laboratory, ETH Zürich, Mattenstrasse 26, CH-4058 Basel, Switzerland

## Supporting Information

**ABSTRACT:** We present an optimized protocol to encapsulate bacteria inside giant unilamellar lipid vesicles combined with a microfluidic platform for real-time monitoring of microbial growth and production. The microfluidic device allows us to immobilize the lipid vesicles and record bacterial growth and production using automated microscopy. Moreover, the lipid vesicles retain hydrophilic molecules and therefore can be used to accumulate products of microbial biosynthesis, which we demonstrate here for a riboflavin-producing bacterial strain. We show that stimulation as well as inhibition of bacterial production can be performed through the liposomal membrane simply by passive diffusion of inducing or antibiotic compounds, respectively. The possibility to introduce as well as accumulate compounds in liposomal cultivation compartments represents great advantage over the current state of the art systems, emulsion droplets, and gel beads. Additionally, the encapsulation of bacteria and monitoring of individual lipid vesicles have been accomplished on a single microfluidic device. The presented system paves the way toward highly parallel microbial cultivation and monitoring as required in biotechnology, basic research, or drug discovery.

**KEYWORDS:** antibiotics, microfluidics, microbiology, liposomes, giant unilamellar vesicles (GUV)



## 1. INTRODUCTION

Microbial cells and their monitoring in a controlled environment are of great importance for biotechnology and drug discovery as well as in basic research. Microbes are the standard host for protein and metabolic engineering<sup>1</sup> by rational design or directed evolution.<sup>2</sup> Microbial cell factories can be used for the production of structurally demanding natural products for the pharmaceutical and chemical industry. The importance and variety of applications for microbes in research and industry nourishes interest in versatile cultivation strategies and complementary sensitive analytical systems.<sup>3,4</sup>

Typical tools for monoseptic cultivations are shake flasks, Petri dishes, bioreactors, and multiwell plates. Petri dishes and shake flasks are straightforward to use but provide only limited control over cultivation conditions, and assays are performed in a low throughput. Bioreactors allow for the regulation of cultivation parameters such as pH, oxygen concentration, or nutrient availability, but they suffer from difficulties to parallelize workflows. Multiwell plates with well numbers of up to more than a thousand offer low volumes and minimal sample consumption and are suited for handling highly parallel cultivation, for example, for drug discovery and toxicity testing.<sup>5</sup> However, automation of liquid handling by pipetting robots is required in order to realize the potential.

A promising strategy for highly parallelized cultivation and automated analysis has emerged with the recent developments of microfluidic systems. Microfluidic devices with cell trapping features have been implemented in microfabricated chambers

of volumes in the range of nL to pL for capturing of single or few cells followed by monitoring of growth and phenotypic characterization.<sup>6–9</sup> For serial analysis at higher throughput, hydrogel microparticles<sup>10–13</sup> and microemulsions<sup>14–19</sup> or double emulsions<sup>20,21</sup> are appealing solutions and can be prepared in microfluidic devices at up to kHz frequencies and with excellent monodispersity to guarantee reproducible conditions.<sup>22</sup> Encapsulated microbial cells can be directly analyzed or incubated for several weeks.<sup>23</sup> Nevertheless, these approaches have some limitations. Thus, in microemulsions, the aqueous culture compartment is surrounded by oil and a surfactant to stabilize the water–oil interface. While the microbes are stably retained inside the aqueous phase, the addition or exchange of compounds including nutrients is difficult. Droplet fusion or so-called picoinjection facilitates the addition of a fluid at one point in time, but controlled feeding over time is not possible.<sup>24,25</sup> Consequently, the culture conditions vary over time. Gel/agarose microparticles on the other hand allow continuous exchange of the nutrients and reagents through diffusion but do not retain small molecules.<sup>26,27</sup>

Recently, others explored the possibility to use lipid vesicles as culture compartments<sup>28–32</sup> to address some limitations of the techniques described above. Giant unilamellar vesicles

Received: July 11, 2019

Accepted: August 27, 2019

Published: August 27, 2019

(GUVs) are composed of a phospholipid membrane and have typically diameters of a few micrometers. They resemble the plasma membrane of living cells and present a biomimetic alternative to isolate and protect encapsulated microbes instead of the oil phase surrounding microemulsion. Nevertheless, the described encapsulation protocols required the use of unphysiologically high sugar concentrations<sup>29–32</sup> in order to achieve density differences required for the GUV preparation, which do not comply with standard cultivation conditions for microbial cultures.

Here, we significantly advanced these initial studies by optimizing the water-in-oil transfer method used for the formation of bacteria-encapsulating GUVs. Instead of using high-density sugar solutions, we opted for a bioinert density gradient medium. Further, we present a microfluidic platform (i) allowing to separate individual GUVs and protect them from the shear stress, (ii) enabling rapid and controlled reagent exchange during the cultivation, and (iii) facilitating real-time monitoring of individual bacteria-encapsulating GUVs via microscopy. Moreover, we successfully demonstrated the possibility to not only cultivate *Escherichia coli* using the presented platform but also furthermore interfere with the bacterial production using the membrane permeable compounds. Finally, to form bacteria-encapsulated GUVs in a more controlled and rapid way, we integrated GUV production, encapsulation, and monitoring of the bacterial cells on a single microfluidic device. Based on the combination of the names *bacteria* and *vesicles*, we refer to the liposomal compartment in its inoculated state as a *basicle*.

## 2. EXPERIMENTAL SECTION

**2.1. Materials.** Anhydrotetracycline hydrochloride (aTC, analytical standard), bovine serum albumin (BSA), OptiPrep (iodoxanol), LB broth, mineral oil, 1-octanol, and polyvinyl alcohol (PVA) were purchased from Sigma-Aldrich. Dulbecco's phosphate-buffered saline (PBS) was purchased from Gibco (Thermo Fisher Scientific). Pluronic F-68 surfactant was purchased from Thermo Fisher Scientific. Polydimethylsiloxane (PDMS) Sylgard 184 was purchased from Dow Corning. Glycerol was purchased from ABCR. 1-Palmityl-2-oylphosphatidylcholine (POPC), 1,2-dioleoyl-*sn*-glycero-3-phosphocholine (DOPC), 1,2-dioleoyl-*sn*-glycero-3-phosphoethanolamine-*N*-lissamine rhodamine B sulfonyl (Rho-PE), and cholesterol were purchased from Avanti Polar Lipids. The antibiotics, kanamycin sulfate (100×), was obtained from Gibco (Life Technologies), ampicillin sodium salt was obtained from Sigma-Aldrich, tetracycline hydrochloride (TC), pharmaceutical grade, was purchased from GERBU Biotechnik GmbH.

**2.2. Bacterial Strains.** To monitor bacterial growth inside the liposomal compartments, strain *E. coli* K12 MG1655 [pSEVA271-*sfGFP*] was used.<sup>33</sup> The strain was modified to overexpress the gene for the green fluorescent protein sfGFP, allowing for simplified quantification and observation of the bacteria. The strain was transformed with plasmid pSEVA271-*sfGFP* (lab collection) carrying the *sfGFP* gene. The plasmid was constructed based on plasmid pSEVA271<sup>34</sup> (p15A origin of replication, kanamycin resistance) adding a gene for sfGFP<sup>35</sup> under control of a constitutive promoter (BioBrick part BBA\_J23100).<sup>36</sup> For riboflavin secretion, strain *E. coli* BW23474 [pB2-*ribDBECA-mkate2*]<sup>37</sup> carrying plasmid pB2-*ribDBECA-mkate2* (p15A origin of replication, kanamycin resistance) was used.<sup>38</sup> The strain overexpresses the genes for riboflavin biosynthesis (*ribDBECA*) arranged in a gene cluster and under control of promoter  $P_{\text{tet}}$ . Riboflavin is produced and secreted under standard cultivation conditions, but levels of riboflavin can be increased by induction of cluster expression using anhydrotetracycline hydrochloride at a concentration of 50 ng mL<sup>-1</sup>.

Bacterial strains were streaked on agar plates (BD Difco LB agar, Miller, Thermo Fisher Scientific). Unless otherwise mentioned, plates and liquid cultures were supplemented with appropriate antibiotics (50  $\mu\text{g mL}^{-1}$  kanamycin sulphate) for plasmid maintenance. For experiments, a liquid preculture was prepared by inoculating 2 mL LB media with a single colony picked from the agar plate. The liquid culture was grown at 37 °C and on a shaking incubator (IKA Shakers) with a shaking speed of 200 rpm. Once the OD<sub>600</sub> of the liquid culture reached 0.4–0.6, the culture was diluted to OD<sub>600</sub> = 0.2 (BW23474 [pB2-*ribDBECA-mkate2*]) or OD<sub>600</sub> = 0.1 (K12 MG1655 [pSEVA271-*sfGFP*]) with fresh LB medium and stored on ice until further processing.

For the on-chip production of bacteria-encapsulating lipid vesicles, a liquid preculture was prepared by inoculating 2 mL of the inner aqueous phase (IA, LB supplemented with 15 vol % glycerol) with a single colony picked from the agar plate. The overnight preculture was diluted to the final OD<sub>600</sub> of 0.4 in fresh IA and introduced into the microfluidic device.

**2.3. Formation of *Basicles*.** *Basicles* were prepared following an adapted protocol for GUVs.<sup>39</sup> We overlaid 500  $\mu\text{L}$  of Dulbecco's PBS (pH 7.0–7.3) with 200  $\mu\text{L}$  mineral oil, wherein we dissolved POPC and cholesterol in a molar ratio 2:1 (total lipid concentration = 200  $\mu\text{M}$ ). Thereby, an oil–water interface was formed. We left the interface for ~12 h at 21 °C to let the amphiphilic lipids rearrange at the interface. In a second tube, we prepared a water-in-oil emulsion that serves as the inner solution of the *basicles*. Here, we used an overnight culture of *E. coli* which was freshly diluted to OD<sub>600</sub> 0.1 (or 0.2 in case of BW23474 [pB2-*ribDBECA-mkate2*]) in LB media containing 50  $\mu\text{g mL}^{-1}$  kanamycin sulphate as the aqueous phase. Additionally, we added 5 vol % of the density gradient medium OptiPrep to a final volume of 50  $\mu\text{L}$  that represented the inner solution. The inner solution was overlaid with 500  $\mu\text{L}$  mineral oil containing dissolved lipids (total lipid concentration = 200  $\mu\text{M}$ , POPC/cholesterol = 2:1). The tube was mechanically agitated to emulsify the inner solution in the oil. The POPC (and cholesterol) present in the mineral oil stabilized the resulting emulsion. The emulsion was transferred to the first tube containing the interface. We used centrifugal forces (1500g for 3 min in an Eppendorf MiniSpin centrifuge) to pass the emulsion droplets through the interface. By passing through the oil–water interface, the outer lipid leaflet forms around the droplets, resulting in GUVs with encapsulated bacteria (=basicle). OptiPrep inside the *basicles* increased their density relative to the outer buffer (here Dulbecco's PBS). Therefore, intact *basicles* sedimented during centrifugation and could be harvested as a pellet. The supernatant was discarded, and the pellet was resuspended with fresh Dulbecco's PBS. This washing process was repeated twice to remove nonencapsulated bacteria and debris.

**2.4. Chip Fabrication.** Observation of individual *basicles* was facilitated by the two-layered microfluidic device shown in Figure S1. A bottom layer contained fluidic channels and array of chambers with hydrodynamic traps. The presented device configuration allows for the capture of 224 vesicles in total, with 32 chambers and 7 trapping sides per chamber. The top layer of the device contained channels which upon pressure induced actuation that served as a valve system. The device is conceptually similar to previously published devices and allows capturing of single vesicles.<sup>40,41</sup> The device consisted of PDMS (1–10 ratio of curing agent and polymer). For the top layer, we casted the PDMS onto the SU-8 mould on a 4 in. silicon wafer and cured the PDMS for approximately 3 h at 80 °C. For the thinner bottom layer, we applied a ~40  $\mu\text{m}$  thick layer of PDMS on a second SU-8 mould by spin-coating and left it to cure for about 1 h at 80 °C. The cured layers were aligned and bonded together by using an intermediate layer of curing agent. Using biopsy punchers, we pierced holes through the PDMS device that we used as inlets or outlets. Finally, the PDMS was bonded to a glass support (Menzel Microscopes Coverslips) with a thickness of about 300  $\mu\text{m}$ . We filled all channels of the microfluidic devices with PBS containing 4 wt % BSA prior to the experiments. Thereby, the microfluidic channels were coated with BSA which prevented vesicles from bursting upon contact with the glass or PDMS.

**2.5. Chip Operation and Imaging.** We mounted the microfluidic chip on an automated, inverted microscope with temperature control. The environmental box was preheated to 37 °C and kept on this temperature during the entire experiment. We filled reservoirs of the microfluidic device with the 20  $\mu\text{L}$  of *basicles* in buffer and supplied the solution by suction into the chip at a flow rate of 1  $\mu\text{L min}^{-1}$ . To wash out free bacteria and nontrapped vesicles, we withdrew about 10  $\mu\text{L}$  of fresh PBS at 1  $\mu\text{L min}^{-1}$ . Then, the donut-shaped valves were closed with 2.6 bar  $\text{N}_2$ . During imaging, we kept flushing fresh buffer through the channels at a flow rate of 0.2–0.5  $\mu\text{L min}^{-1}$  to avoid bubble formation. Reagents were exchanged by pipetting the new solution (i.e., inducer or antibiotics) into the chip reservoirs and withdrawing the solution into the chip (1–2  $\mu\text{L min}^{-1}$ ) while the donut-shaped valves were closed. When the fresh solution surrounded all of the chambers, the pressure was decreased to 1–1.5 bar to partially open the donut valves. Valves remained open for about 10 s and were closed by increasing the pressure again. The process was repeated three times with about 1 min waiting time in between. This ensured that the solution in the chambers was exchanged without being diluted by the previous solution and the solution released during this exchange. During the exchange, new solution was continuously supplied. Inducer and antibiotics were diluted in the PBS containing 4 wt % BSA. We imaged each of the individual chambers with the trapped *basicles* every 30 min using brightfield and fluorescence microscopy on a fully motorized inverted wide-field microscope (Nikon Ti-Eclipse) through a 20 $\times$  objective (Nikon, S Plan Fluor ELWD 20 $\times$ ). We used a Lumencor Spectra X LED light source for fluorescence excitation with appropriate optical filters and dichroic mirrors (green channel: cyan LED, 475/28 excitation filter, 495 dichroic, 525/50 emission filter; red channel: green LED, 549/15 excitation filter, 562 dichroic, 593/40 emission filter). Images were recorded by a Hamamatsu Orca Flash 4 camera (exposure times: 50 ms bf, 100 ms green and red). We recorded images of the *basicles* for 10 h. The microscope was driven by NIKON NIS-Elements Advanced Research software, and images were acquired using the Nikon Perfect Focus System.

**2.6. Microfluidic Device for On-Chip *Basicle* Production.** We used a two-layered microfluidic device similar to the device described above. Here, the fluidic layer additionally contained a double-emulsion forming junction<sup>21</sup> placed upstream of the GUV trapping array (in total, 72 traps and chambers). The pressure layer contained donut-shaped valves, identical to previously described microfluidic valves. The device has three fluidic inlets for the outer aqueous phase (OA), the lipid-containing octanol phase (LO), and the inner aqueous phase (IA), with one outlet placed after the trapping array. The channels for the OA and the trapping array as well as the channel between them were selectively coated with 2.5 wt % PVA solution to increase their hydrophilicity. The IA and LO channels were protected with the positive air pressure during the PVA coating process and remained hydrophobic.<sup>42</sup> The PVA coating layer was cured for about 30 min at 120 °C.

**2.7. On-Chip Production of Lipid Vesicles with Encapsulated Bacteria.** The on-chip production of GUVs started with the formation of monodispersed LB-in-octanol-in-LB double emulsions in which bacteria were encapsulated. The microfluidic encapsulation of bacteria in double emulsions follows the Poisson distribution, and we found an initial  $\text{OD}_{600}$  of 0.4 to be ideal to obtain predominantly *basicles* with a single bacterium. Consequently, a high number of GUVs is not inoculated and few *basicles* contain two or three bacteria.

Culture media supplemented with 15 vol % glycerol forms the IA phase of the double emulsion, while the OA phase additionally contains 5 vol % of Pluronic F-68 surfactant. Octanol with dissolved lipids, DOPC/Rho-PE 99.9:0.1 mol % in 1-octanol (2 mg  $\text{mL}^{-1}$  total lipid concentration), forms an octanol shell (LO). The fluid flow was controlled using the Fluigent pressure control unit with separate pressure channels connected to vials containing IA, LO, and OA. The pressures were set to  $\sim$ 15 mbar for IA and LO and 100–120 mbar for OA. To establish a stable double emulsion production, the pressure-driven flows of the IA and LO were adjusted during the production if necessary to account for possible fluctuations. Once the traps were

sufficiently filled with *basicles*, the pressures applied at the IA and LO vials were set to zero, and the GUV formation was stopped. We actuated the microfluidic valves by using the Fluigent pressure control unit to apply pressure to the control channel and thereby isolated individual vesicles.

For better visualization and therefore control of the formation process, we added a fluorescently labeled lipid, Rho-PE to the LO. The fluorescent label allowed us to visually confirm the proper vesicle formation and distinguish formed membranes from the octanol droplets. The on-chip production of bacteria-encapsulating vesicles was performed at 25 °C. The temperature was increased to 37 °C, and individual vesicles were monitored using fluorescence microscopy for up to 15 h. We used the same wide-field microscope (Nikon Ti-Eclipse) as described previously with a 40 $\times$  objective (Nikon, S Plan Fluor ELWD 40 $\times$ ).

**2.8. Data Analysis.** Microscopy images were processed and analyzed in FIJI image analysis software. Circular regions of interest (ROIs) were selected around the analyzed *basicle*, and the grey values were measured. The obtained data were processed and plotted in MATLAB (MathWorks). We performed background subtractions in all images. We calculated the mean integrated density (sum of all grey values in ROI) of the measured GFP and mKate2 fluorescence. In the case of secreted riboflavin, we calculated the mean intensity (mean grey value of pixels in a ROI) as it represented a concentration. For the data graphs, we calculated and plotted the 95% bootstrap confidence interval (calculated from 1000 bootstrap samples).

The mean normalized riboflavin production per biomass was calculated by dividing the riboflavin fluorescence with the respective mKate2 fluorescence for each individual vesicle at each time point after the background extraction. Empty GUVs, damaged *basicles*, or overlapping *basicles* were omitted from the analysis.

The bacterial number was approximated by converting the images to RGB 8-bit and subtracting the background. After further application of the threshold (selection of the cut off pixel intensity value to distinguish between fluorescence signal and background) and watershed segmentation, particle analysis plugin from FIJI software was used.<sup>43</sup>

### 3. RESULTS AND DISCUSSION

Bacteria were encapsulated in the GUV cultivation compartments using an optimized water-in-oil transfer method. It is crucial for this method that the bacteria-containing IA phase of the vesicles is denser than the OA phase, PBS. We opted to use OptiPrep (iodixanol) as a bioinert high-density agent instead of the commonly used glucose/sucrose solution. OptiPrep is osmotically inactive therefore there was no need to balance osmolarity of the outer solution. We further confirmed that OptiPrep has no major impact on cell growth (Figure S2) and on vesicle stability compared to GUVs prepared with glucose/sucrose solutions (data not shown). This modification of the protocol allowed us to cultivate bacteria inside the liposomes at conditions similar to the standard bacterial cultures.

First, we diluted bacteria in media containing 5 vol % OptiPrep and overlaid the bacterial culture with mineral oil containing the phospholipid POPC as a 2:1 mixture with cholesterol. A water-in-oil emulsion was formed by mechanical agitation of the two phases (Figure 1a). The emulsion was transferred onto a lipid-stabilized oil–water interface prepared in a second tube. Having the highest density, the emulsion passed through the interface during centrifugation. Thereby, a stable lipid bilayer was formed around the bacteria-encapsulating aqueous compartment (Figure 1b), and the resulting *basicles* were collected at the bottom of the tube.

Shortly after formation, we introduced *basicles* into a microfluidic device and observed them for typically 10 h and up to 15 h. The microfluidic device made of PDMS consisted

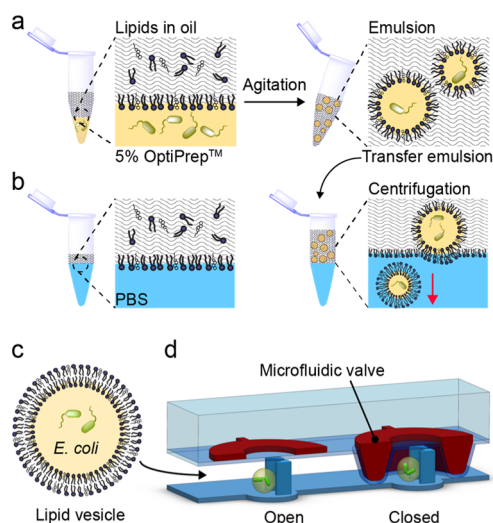


**Figure 1.** (a) Bacterial culture supplemented with OptiPrep (yellow) was emulsified in mineral oil-containing phospholipids and cholesterol. The lipids stabilized the emulsion. (b) Water–oil interface was created in a second tube. Phospholipids aligned at the interface. The emulsion formed previously was carefully added to the oil phase. By centrifuging, the OptiPrep-containing emulsion passed through the interface and buffer (blue). Thereby, GUVs that encapsulate bacteria were formed. (c) Bacteria encapsulated in a GUV. (d) Side perspective view of hydrodynamic traps with *basicles*, isolated by a microfluidic valve. The valve is closed when the top channel (red) is actuated and deflects a PDMS membrane. Without actuation in the control channel, the valve is open.

of a channel network with implemented hydrodynamic traps (Figure S1).<sup>40</sup> The traps could be separated from the flow by actuating round valves located above the trapping sites (Figure 1d). This particular design allowed us to stably immobilize individual GUVs at predefined locations which facilitated automated imaging and provided temporal and spatial control over the exchange of fluids. Additionally, *basicles* were protected from shear stress during the cultivation. The mean diameter of monitored *basicles* was around 12  $\mu\text{m}$  (Figure S3), given by the 5  $\mu\text{m}$  gap of the hydrodynamic traps and the channel height of 20  $\mu\text{m}$ . Prior to cultivation, trapped *basicles* were washed with PBS and nontrapped *basicles* and bacteria were removed.

In initial experiments, we aimed to demonstrate that bacteria sustain the preparation of the *basicles* unharmed and that *basicles* serve as a liposomal compartment. We expected that the water-soluble carbon sources in LB media (peptides and amino acids) will not passively diffuse through the membrane,<sup>44,45</sup> allowing bacteria to grow within GUVs for multiple generations. To confirm this, we selected the well-characterized laboratory strain, *E. coli* (K12 MG1655), capable of producing sfGFP which also serves as an arbiter for biomass quantification by fluorescence microscopy. We collected fluorescence images of individual *basicles* cultivated on the microfluidic device every 30 min over 10 h period. The mean sfGFP fluorescence per GUV is shown in Figure 2 along with time-lapse images of a selected *basicle*.

An estimation of the number of bacteria inside the selected GUV based on the fluoresce intensity and automated particle counting is presented in the inset graph, Figure 2a. The count starts at zero as the initial fluorescence intensity of the bacteria was below the set threshold. Similarly, for the consecutive frames, the number of detected bacteria fluctuates. Bacteria are freely moving inside the GUV, and temporarily overlapping cells (in z-direction) as well as out-of-focus cells are difficult to distinguish by the automated image analysis. Nevertheless, we clearly observed an increasing trend with about 18 cells after the 10 h cultivation, corresponding to approximately four generations. Also, the increase of the mean sfGFP fluorescence is positively correlated with the increase of the number of bacteria per GUV observed visually (Figures 2b and S4, Movie S1) and using automated particle counting. The results clearly indicate the increase of biomass, suggesting that no essential compounds leaked out of the GUVs and nutrients were accessible to the bacteria inside GUVs to grow and divide in the expected rate. At the same time, we did not observe the growth of the bacteria outside of the *basicles*, confirming a lack of nutrients outside of the GUVs (see Figure S5). The width of the confidence interval reflects the variation of the fluorescence intensity between individual colonized GUVs. These differences resulted from heterogeneities between bacteria; variations in the initial number of bacteria per vesicle and the volume of GUVs contributed to these variations as well. We found that GUVs were stable for up to 15 h in conventional cultivation conditions (temperature, buffer, and media). Furthermore, we confirmed that *basicles* can be analyzed using flow-cytometry. Based on sfGFP fluorescence,

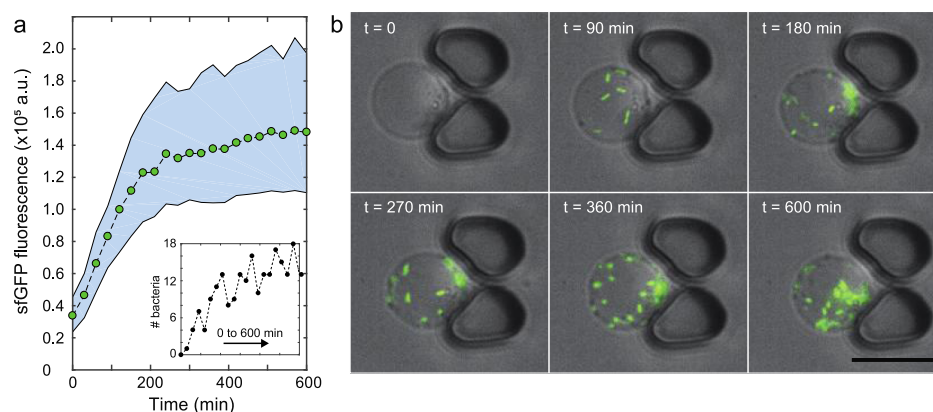


**Figure 2.** Bacterial growth and sfGFP production of *E. coli*. (a) Mean sfGFP production per GUV with 95% confidence interval ( $n = 12$ ). The inset depicts the estimated cell number in the GUV shown in (b). Here, the bacterial count starts at zero due to the low fluorescence intensity in the first frame. (b) Time-lapse images of a GUV-encapsulating sfGFP producing bacteria. Scale bar = 25  $\mu\text{m}$ .

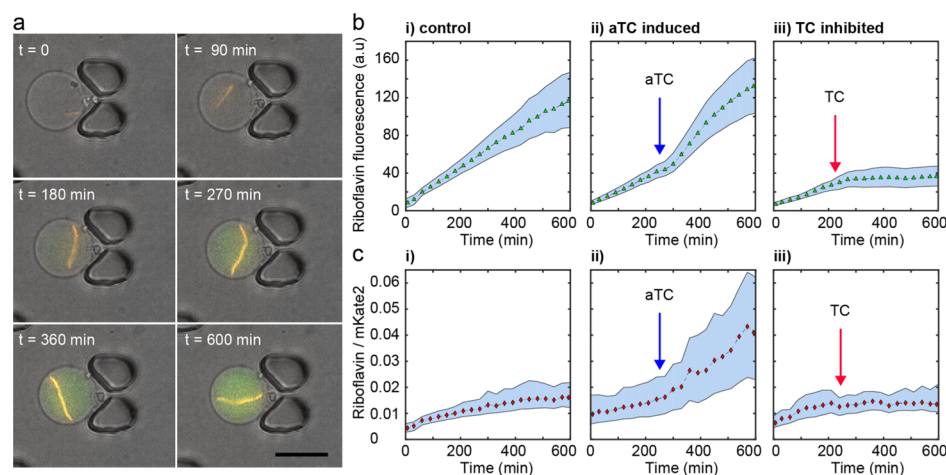


**Figure 3.** Riboflavin production of *E. coli*. (a) Time-lapse images of a GUV encapsulating a riboflavin (green) producing bacterium (red). Scale bar = 25  $\mu\text{m}$ . (b) Mean riboflavin production (triangle) of GUVs with 95% confidence interval cultivated under three different conditions: (i) without exchange of reagents, (ii) induced with anhydrotetracycline hydrochloride (aTC) after 240 min of standard growth, and (iii) supplemented with tetracycline hydrochloride (TC) after 240 min. (c) Riboflavin fluorescence intensity (from b) normalization to the respective biomass (derived from mKate2 fluorescence) with 95% confidence interval in blue ( $n_i = 15$ ,  $n_{ii} = 14$ ,  $n_{iii} = 15$ ).

we identified empty GUVs, free bacteria (i.e. not encapsulated), and *bacilles* with negative, low, and bright fluorescence intensity, respectively (Figure S6).

We further demonstrate the possibility to accumulate a biosynthesized product inside the GUVs and the possibility to interfere with the biosynthesis pathway of microbial cells by adding membrane-permeable compounds. We selected an *E. coli* (BW23474) strain which overexpresses certain genes of the riboflavin (vitamin B<sub>2</sub>) biosynthesis pathway production and secretes the vitamin. Riboflavin exhibits green fluorescence and could be monitored by fluorescence microscopy. To quantify the biomass, we additionally equipped the strain with the red-fluorescent protein mKate2 (see Figure S7).

To compare the riboflavin production under the different conditions, we plotted the increase of the mean riboflavin fluorescence over the cultivation period. Additionally, we estimated the slope of the riboflavin accumulation by approximation as a linear function (see Figure S8a). As a measure for the cellular response toward selected membrane-permeable compounds, we investigated the mean normalized riboflavin production per biomass, calculated as ratio of riboflavin and mKate2 fluorescence (Figure S8b).

We were able to observe secretion and accumulation of riboflavin inside GUVs. Figure 3a shows time-lapse images of growth/elongation of an encapsulated bacterium (red) and the secretion of riboflavin (green) (see also Figure S9 and Movie S2). Riboflavin production resulted in a less frequent separation of dividing cells which led to elongation and filamentous morphology. The same morphology was observed in the shake-flask culture (data not shown), that is, the irregular shape is not due to the cultivation in the GUVs but due to stress resulting from riboflavin overexpression. Geometric restrictions by the lipid membrane resulted in bending of elongated bacteria (Figure S10, Movie S3); the deformation of lipid vesicles due to the continuous elongation of filaments was observed very rarely.

The mean riboflavin fluorescence measured in GUVs is represented in Figure 3bi. Riboflavin accumulates linearly with an estimated slope of 0.17–0.19 a.u. per min. During the 10 h cultivation, the riboflavin fluorescence does not reach a plateau, and the green fluorescence outside of GUVs remains

constant (data not shown). Therefore, we conclude that the GUV efficiently retained riboflavin inside and leakage through the lipid membrane was negligible.

Riboflavin was produced and accumulated at a rather constant rate as the cells were growing as is reflected by the normalized mean riboflavin production (Figure 3ci). The normalized riboflavin fluorescence remained in the range between 0.005 and 0.015 throughout the cultivation period, showing that the riboflavin level increased along with the biomass (mKate2 fluorescence).

The significant advantage of the presented system is that membrane-permeable reagents can be supplied at any selected time point by passive diffusion across the liposomal membrane, whereas the response of the encapsulated bacteria can be monitored on the individual GUV level. Previous studies showed that tetracyclines permeate passively through lipid membranes.<sup>20</sup> Therefore, tetracyclines were ideal candidates to confirm whether compounds could be supplied to the liposomal encapsulated bacteria from the outer media. Anhydrotetracycline hydrochloride (aTC) is an inducer of the gene cluster responsible for the riboflavin biosynthesis, and tetracycline hydrochloride (TC) is a known bacteriostatic antibiotic. TC inhibits the ribosomal translation and therefore protein production and growth of bacteria.

First, we cultivated the riboflavin-producing bacteria in GUVs in the absence of tetracyclines for 240 min to ensure that bacteria adapted to the environment indicated by the increase of biomass (mKate2) and riboflavin fluorescence. Subsequently, we replaced the buffer surrounding the *bacilles* with a buffer containing 50 ng mL<sup>-1</sup> aTC or 100  $\mu\text{g mL}^{-1}$  TC, respectively. For this, we shortly opened the microfluidic valves. Afterward, the cultivation was continued with either aTC or TC present.

Directly after the induction by aTC, the riboflavin production evidently changed as seen in Figure 3bii. As indicated by the fluorescence intensity, directly after the induction by aTC, riboflavin production increased from 0.13 to approximately 0.29 a.u. per min (Figures 3bii; S6). The results indicate that in comparison to uninduced cells, more riboflavin was secreted per time unit as well as per relative biomass. Moreover, the normalized riboflavin fluorescence (Figure 3cii)

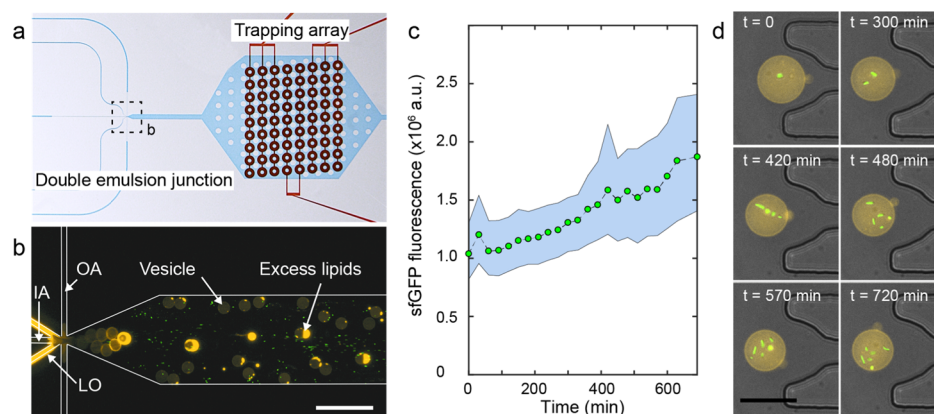


**Figure 4.** On-chip production and monitoring of the *basicles*. (a) Integrated microfluidic device for production and monitoring of *basicles* with fluidic channels (blue) and microfluidic valves (red). (b) Formation of *basicles* at the channel junction. IA: inner aqueous phase (bacterial suspension), OA: outer aqueous phase, LO: lipids in 1-octanol. Scale bar = 100  $\mu\text{m}$ . (c) Mean sfGFP production per *basicle* with 95% confidence interval ( $n = 10$ ). (d) Time-lapse images of a selected rhodamine-labeled *basicle* (yellow) with sfGFP producing bacteria (green). Scale bar = 25  $\mu\text{m}$ .

increased to 0.04 toward the end of the cultivation and more than doubles after 10 h, exceeding the values recorded for cells without the aTC supplement.

In contrast, riboflavin production instantaneously decreased in *basicles* that had been exposed to TC (Figure 3biii). The estimated slopes of the riboflavin fluorescence decreased from 0.1 to 0.006 a.u. per min (Figure S8). After the TC supplement, the normalized riboflavin production remained in a comparable range as for cells cultivated in the absence of tetracyclines (Figure 3ciii). These results indicate that TC-exposed cells discontinued to grow as well as produce riboflavin. The biomass and produced riboflavin per vesicle remained approximately at the level of the last time point before the TC exposure. Neither the biomass nor riboflavin level increased for the rest of the 10 h cultivation period.

Taken together, these observations corroborate that amphiphilic compounds supplied from outer buffer permeated into the GUVs and qualitatively affected the growth behavior of the strain and its riboflavin biosynthesis behavior as expected. The effect of the inducer, aTC, and growth inhibiting TC on the bacterial cultivation was further confirmed by microplate reader experiments, without the presence of lipid vesicles (Figure S11).

Additionally, the combination of the presented cultivation system with the microfluidic device allows different bacterial strains to be cultivated together in one microfluidic chamber and hence under the same conditions (Figure S12). Both strains are isolated in their liposomal membrane without the risk of cross-contamination. Similarly, *basicles* containing both different bacterial strains were prepared as well (Figure S13), showing the potential of the presented protocol for different applications.

In the next step, we combined the formation of GUVs with encapsulated bacteria followed by their capture on a single microfluidic device (Figure 4a). This method to form GUVs introduced by the Dekker group<sup>21,42</sup> is based on the microfluidic formation of a double-emulsion in a six-way junction. An IA phase is surrounded by the lipid-carrying organic phase (LO) and subsequently pinched off by the stream of the OA phase. The OA and IA phases contain 15 vol % glycerol to increase viscosity of the aqueous solutions to help improve the pinch off process and stabilize formed interfaces.

Additionally, the OA phase contained 5 vol % Pluronic F-68 surfactant to prevent coalescence of double-emulsion droplets and improve their stability. Key for the subsequent formation of GUVs is a dewetting process in which an excess organic phase accumulates at the front of the double-emulsion droplet before budding off as a smaller octanol droplet and leaving behind a lipid bilayer. Previous works from Deshpande et al.<sup>21,46</sup> confirmed that the produced GUVs are unilamellar by successfully incorporating the bilayer-spanning  $\alpha$ -hemolysin pore in the on-chip produced GUVs.

We adopted this method to encapsulate bacteria inside GUVs and monitor their growth and production using the presented microfluidic device. The experiments were performed with the organic phase containing DOPC and 0.1 mol % fluorescent Rho-PE to monitor proper GUV formation. Bacterial culture supplemented with 15 vol % glycerol formed the IA phase; the OA phase additionally contained 5 vol % of Pluronic F-68 surfactant. Once a bacteria-containing double emulsion was formed in the junction, dissolved lipids started to assemble at the water–octanol interface. Excess lipids and octanol partially separated as a prominent pocket at the front of the droplet due to a dewetting process. The pocket eventually completely detached, creating an unilamellar lipid vesicle containing encapsulated bacteria (Figure 4b). Freshly produced lipid vesicles traveled together with the detached octanol droplets toward the trapping array. Hydrodynamic traps were designed such that small and flexible octanol droplets passed between the posts (gap = 9.5  $\mu\text{m}$ ) while lipid vesicles between 10 and 30  $\mu\text{m}$  in diameter (depending on the applied pressures) remained inside the trap. The *basicles* are captured at the trapping array and monitored. The mean sfGFP fluorescence together with the time-lapse image of a selected GUV is shown in Figure 4c,d and S14. The sfGFP fluorescence (biomass) was continuously increasing over the cultivation period (11 h), clearly showing that bacteria grow and divide in the produced GUVs. With this, we successfully demonstrated for the first time a streamlined workflow of encapsulating *E. coli* in GUVs with subsequent trapping and monitoring. Even though *E. coli* can use glycerol as a carbon source, higher concentrations can lead to osmotic stress; therefore, we currently test potential replacements for glycerol to provide cultivation conditions even closer to conditions

typically used. Moreover, significantly less or no residual oil is left in GUV membranes,<sup>21,42</sup> potentially allowing better incorporation of membrane proteins, important for future direction and usability of the *basicle* concept.

#### 4. CONCLUSIONS

In summary, we demonstrated that lipid vesicles are versatile culture compartments for the monoseptic cultivation of bacteria combining advantages of both droplets and gel beads. Similar to droplets, the presented system encloses single to few microbes and retains hydrophilic products while additionally offers possibility to supply membrane-permeable stimulants during the cultivation through the aqueous media. The first presented technique for *basicle* formation is an excellent tool for simple and fast bacterial encapsulation without the need of a special equipment. These *basicles* can be introduced in a microfluidic device with integrated traps for monitoring and rapid, selective fluid exchange.

Moreover, we showed on-line *basicle* formation and trapping, opening the possibility for high throughput production and parallel studies for a variety of microbial cultures. The integrated microfluidic preparation of *basicles* is rapid and well controlled regarding the size and composition of the GUVs, which is crucial in comparative studies. The formation process, however, requires the use of glycerol and the Pluronic surfactant, which may influence the membrane permeability of compounds as well as assays within the *basicles*.

We believe that *basicles* have the potential to support or even replace currently used microfluidic cultivation compartments as are microemulsions and gel beads. Further, the unique properties of the lipid membrane allow employing cell-biological systems (membrane pores, membrane-bound transporters) to further tailor membrane permeability, for example, accumulation of the product of bacterial biosynthesis, while releasing and therefore diluting toxic byproducts or replenish depleted nutrients through membrane pores. We are convinced that the technique will become a powerful tool for rapid screening and parallel observation of monoclonal microbial cultures, for example, for drug discovery or testing.

#### ■ ASSOCIATED CONTENT

##### Supporting Information

The Supporting Information is available free of charge on the ACS Publications website at DOI: 10.1021/acsami.9b12169.

Materials and methods and supplementary figures (PDF)

MOV\_1: GUV encapsulating sfGFP-producing *E. coli* (AVI)

MOV\_2: GUV encapsulating riboflavin-secreting (green fluorescence) *E. coli* (BW23474), 15 h. The bacteria produced mKate2 (red) constitutively (AVI)

MOV\_3: Time-lapse movie of a bacteria (BW23474) growing inside a GUV (AVI)

MOV\_4: Growth and production of two *E. coli* strains, MG1655 (outside, green) and BW23474 (vesicle, red) (AVI)

#### ■ AUTHOR INFORMATION

##### Corresponding Author

\*E-mail: [petra.dittrich@bsse.ethz.ch](mailto:petra.dittrich@bsse.ethz.ch).

##### ORCID

Steven Schmitt: 0000-0001-9492-8958

Petra S. Dittrich: 0000-0001-5359-8403

##### Author Contributions

#P.J. and Y.R.F.S. contributed equally.

##### Author Contributions

P.J. and Y.R.F.S. contributed equally. P.J. and Y.R.F.S. performed the experiments and evaluated the data. P.J., Y.R.F.S., and P.S.D. developed the concept and wrote the manuscript. A.S. performed on-chip production experiments. S.S. provided the recombinant bacteria and provided support during manuscript writing. M.H. and P.S.D. supervised the project. The manuscript was written through contributions of all authors. All authors approved the manuscript.

##### Notes

The authors declare no competing financial interest.

#### ■ ACKNOWLEDGMENTS

The financial funding of the Swiss National Foundation SNF NRP72, project 407240\_167123 and NCCR Molecular Systems Engineering's and the European Research Council (ERC Consolidator grant no. 681587) is gratefully acknowledged. We thank the Single Cell Facility of the Department BSSE for their help with imaging and image analysis and especially Dr. Mariangela Di Tacchio for performing FACS experiments and analysis. We would like to thank Marion Ort (University of Basel) for the discussions. We are also grateful for the support and help from the clean room facilities of the BSSE, ETH Zurich. We are also grateful for the proofreading by Dr. Darius Rackus (ETH Zurich).

#### ■ ABBREVIATIONS

aTC, anhydrotetracycline hydrochloride  
GUVs, giant unilamellar vesicles  
PDMS, polydimethylsiloxane  
POPC, 1-palmitoyl-2-oleoyl-*sn*-glycero-3-phosphocholine  
sfGFP, green fluorescent protein  
TC, tetracycline hydrochloride

#### ■ REFERENCES

- (1) Keasling, J. D. Manufacturing Molecules Through Metabolic Engineering. *Science* **2010**, *330*, 1355–1358.
- (2) Griffiths, A. D.; Tawfik, D. S. Directed Evolution of an Extremely Fast Phosphotriesterase by in Vitro Compartmentalization. *EMBO J.* **2003**, *22*, 24–35.
- (3) Feng, J.; Wang, T.; Shi, W.; Zhang, S.; Sullivan, D.; Auwaerter, P. G.; Zhang, Y. Identification of Novel Activity against *Borrelia burgdorferi* Persists Using an FDA Approved Drug Library. *Emerging Microbes Infect.* **2014**, *3*, 1–8.
- (4) Courtois, S.; Cappellano, C. M.; Ball, M.; Francou, F.-X.; Normand, P.; Helynck, G.; Martinez, A.; Kolvek, S. J.; Hopke, J.; Osburne, M. S.; August, P. R.; Nalin, R.; Guerineau, M.; Jeannin, P.; Simonet, P.; Pernodet, J.-L. Recombinant Environmental Libraries Provide Access to Microbial Diversity for Drug Discovery from Natural Products. *Appl. Environ. Microbiol.* **2003**, *69*, 49–55.
- (5) Cheng, T.-J. R.; Wu, Y.-T.; Yang, S.-T.; Lo, K.-H.; Chen, S.-K.; Chen, Y.-H.; Huang, W.-L.; Yuan, C.-H.; Guo, C.-W.; Huang, L.-Y.; Chen, K.-T.; Shih, H.-W.; Cheng, Y.-S. E.; Cheng, W.-C.; Wong, C.-H. High-Throughput Identification of Antibacterials against Methicillin-Resistant *Staphylococcus aureus* (MRSA) and the Transglycosylase. *Bioorg. Med. Chem.* **2010**, *18*, 8512–8529.
- (6) Balagadde, F. K.; You, L.; Hansen, C. L.; Arnold, F. H.; Quake, S. R. Long-Term Monitoring of Bacteria Undergoing Programmed Population Control in a Microchemostat. *Science* **2005**, *309*, 137–140.



- (7) Grünberger, A.; Probst, C.; Helfrich, S.; Nanda, A.; Stute, B.; Wiechert, W.; von Lieres, E.; Nöh, K.; Frunzke, J.; Kohlheyer, D. Spatiotemporal Microbial Single-Cell Analysis Using a High-Throughput Microfluidics Cultivation Platform. *Cytometry, Part A* **2015**, *87*, 1101–1115.
- (8) Avesar, J.; Rosenfeld, D.; Truman-Rosentsvit, M.; Ben-Arye, T.; Geffen, Y.; Bercovici, M.; Levenberg, S. Rapid Phenotypic Antimicrobial Susceptibility Testing Using Nanoliter Arrays. *Proc. Natl. Acad. Sci. U.S.A.* **2017**, *114*, E5787–E5795.
- (9) Stratz, S.; Verboket, P. E.; Hasler, K.; Dittrich, P. S. Cultivation and Quantitative Single-Cell Analysis of *Saccharomyces Cerevisiae* on a Multifunctional Microfluidic Device. *Electrophoresis* **2018**, *39*, 540–547.
- (10) Walser, M.; Pellaux, R.; Meyer, A.; Bechtold, M.; Vanderschuren, H.; Reinhardt, R.; Magyar, J.; Panke, S.; Held, M. Novel Method for High-Throughput Colony PCR Screening in Nanoliter-Reactors. *Nucleic Acids Res.* **2009**, *37*, e57.
- (11) Kalyanaraman, M.; Retterer, S. T.; McKnight, T. E.; Ericson, M. N.; Allman, S. L.; Elkins, J. G.; Palumbo, A. V.; Keller, M.; Doktycz, M. J. Controlled Microfluidic Production of Alginate Beads for in Situ Encapsulation of Microbes. In *2009 First Annual ORNL Biomedical Science & Engineering Conference*; IEEE, 2009; pp 1–4.
- (12) Kim, B. J.; Park, T.; Moon, H. C.; Park, S.-Y.; Hong, D.; Ko, E. H.; Kim, J. Y.; Hong, J. W.; Han, S. W.; Kim, Y.-G.; Choi, I. S. Cytoprotective Alginate/Polydopamine Core/Shell Microcapsules in Microbial Encapsulation. *Angew. Chem., Int. Ed.* **2014**, *53*, 14443–14446.
- (13) Meyer, A.; Pellaux, R.; Potot, S.; Becker, K.; Hohmann, H.-P.; Panke, S.; Held, M. Optimization of a Whole-Cell Biocatalyst by Employing Genetically Encoded Product Sensors inside Nanoliter Reactors. *Nat. Chem.* **2015**, *7*, 673–678.
- (14) Brouzes, E.; Medkova, M.; Savenelli, N.; Marran, D.; Twardowski, M.; Hutchison, J. B.; Rothberg, J. M.; Link, D. R.; Perrimon, N.; Samuels, M. L. Droplet Microfluidic Technology for Single-Cell High-Throughput Screening. *Proc. Natl. Acad. Sci. U.S.A.* **2009**, *106*, 14195–14200.
- (15) Jakiela, S.; Kaminski, T. S.; Cybulski, O.; Weibel, D. B.; Garstecki, P. Bacterial Growth and Adaptation in Microdroplet Chemostats. *Angew. Chem., Int. Ed.* **2013**, *52*, 8908–8911.
- (16) Zhang, Y.; Ho, Y.-P.; Chiu, Y.-L.; Chan, H. F.; Chlebina, B.; Schuhmann, T.; You, L.; Leong, K. W. A Programmable Microenvironment for Cellular Studies via Microfluidics-Generated Double Emulsions. *Biomaterials* **2013**, *34*, 4564–4572.
- (17) Weitz, M.; Mückl, A.; Kapsner, K.; Berg, R.; Meyer, A.; Simmel, F. C. Communication and Computation by Bacteria Compartmentalized within Microemulsion Droplets. *J. Am. Chem. Soc.* **2014**, *136*, 72–75.
- (18) Gielen, F.; Hours, R.; Emond, S.; Fischlechner, M.; Schell, U.; Hollfelder, F. Ultrahigh-throughput-directed enzyme evolution by absorbance-activated droplet sorting (AADS). *Proc. Natl. Acad. Sci. U.S.A.* **2016**, *113*, E7383–E7389.
- (19) Shang, L.; Cheng, Y.; Zhao, Y. Emerging Droplet Microfluidics. *Chem. Rev.* **2017**, *117*, 7964–8040.
- (20) Chang, C. B.; Wilking, J. N.; Kim, S.-H.; Shum, H. C.; Weitz, D. A. Monodisperse Emulsion Drop Microenvironments for Bacterial Biofilm Growth. *Small* **2015**, *11*, 3954–3961.
- (21) Deshpande, S.; Caspi, Y.; Meijering, A. E. C.; Dekker, C. Octanol-Assisted Liposome Assembly on Chip. *Nat. Commun.* **2016**, *7*, 10447.
- (22) Theberge, A. B.; Courtois, F.; Schaerli, Y.; Fischlechner, M.; Abell, C.; Hollfelder, F.; Huck, W. T. S. Microdroplets in Microfluidics: An Evolving Platform for Discoveries in Chemistry and Biology. *Angew. Chem., Int. Ed.* **2010**, *49*, S846–S868.
- (23) Mahler, L.; Wink, K.; Beulig, R. J.; Scherlach, K.; Tovar, M.; Zang, E.; Martin, K.; Hertweck, C.; Belder, D.; Roth, M. Detection of Antibiotics Synthesized in Microfluidic Picolitre-Droplets by Various Actinobacteria. *Sci. Rep.* **2018**, *8*, 13087.
- (24) Abate, A. R.; Hung, T.; Mary, P.; Agresti, J. J.; Weitz, D. A. High-Throughput Injection with Microfluidics Using Picoinjectors. *Proc. Natl. Acad. Sci. U.S.A.* **2010**, *107*, 19163–19166.
- (25) O'Donovan, B.; Eastburn, D. J.; Abate, A. R. Electrode-Free Picoinjection of Microfluidic Drops. *Lab Chip* **2012**, *12*, 4029–4032.
- (26) Eun, Y.-J.; Utada, A. S.; Copeland, M. F.; Takeuchi, S.; Weibel, D. B. Encapsulating Bacteria in Agarose Microparticles Using Microfluidics for High-Throughput Cell Analysis and Isolation. *ACS Chem. Biol.* **2011**, *6*, 260–266.
- (27) Duarte, J. M.; Barbier, I.; Schaerli, Y. Bacterial Microcolonies in Gel Beads for High-Throughput Screening of Libraries in Synthetic Biology. *ACS Synth. Biol.* **2017**, *6*, 1988–1995.
- (28) Tan, Y.-C.; Hettiarachchi, K.; Siu, M.; Pan, Y.-R.; Lee, A. P. Controlled Microfluidic Encapsulation of Cells, Proteins, and Microbeads in Lipid Vesicles. *J. Am. Chem. Soc.* **2006**, *128*, 5656–5658.
- (29) Chowdhuri, S.; Cole, C. M.; Devaraj, N. K. Encapsulation of Living Cells within Giant Phospholipid Liposomes Formed by the Inverse-Emulsion Technique. *ChemBioChem* **2016**, *17*, 886–889.
- (30) Morita, M.; Katoh, K.; Noda, N. Direct Observation of Bacterial Growth in Giant Unilamellar Vesicles: A Novel Tool for Bacterial Cultures. *ChemistryOpen* **2018**, *7*, 844.
- (31) Trantidou, T.; Dekker, L.; Polizzi, K.; Ces, O.; Elani, Y. Functionalizing Cell-Mimetic Giant Vesicles with Encapsulated Bacterial Biosensors. *Interface Focus* **2018**, *8*, 20180024.
- (32) Elani, Y.; Trantidou, T.; Wylie, D.; Dekker, L.; Polizzi, K.; Law, R. V.; Ces, O. Constructing Vesicle-Based Artificial Cells with Embedded Living Cells as Organelle-like Modules. *Sci. Rep.* **2018**, *8*, 4564.
- (33) Guyer, M. S.; Reed, R. R.; Steitz, J. A.; Low, K. B. Identification of a Sex-Factor-Affinity Site in *E. Coli* as Gamma Delta. *Cold Spring Harbor Symp. Quant. Biol.* **1981**, *45*, 135–140.
- (34) Silva-Rocha, R.; Martínez-García, E.; Calles, B.; Chavarría, M.; Arce-Rodríguez, A.; de las Heras, A.; Páez-Espino, A. D.; Durante-Rodríguez, G.; Kim, J.; Nikel, P. I.; Platero, R.; De Lorenzo, V. The Standard European Vector Architecture (SEVA): A Coherent Platform for the Analysis and Deployment of Complex Prokaryotic Phenotypes. *Nucleic Acids Res.* **2013**, *41*, D666–D675.
- (35) Pédelacq, J.-D.; Cabantous, S.; Tran, T.; Terwilliger, T. C.; Waldo, G. S. Engineering and Characterization of a Superfolder Green Fluorescent Protein. *Nat. Biotechnol.* **2006**, *24*, 79–88.
- (36) Galagan, J. E.; Calvo, S. E.; Cuomo, C.; Ma, L.-J.; Wortman, J. R.; Batzoglou, S.; Lee, S.-I.; Baştürkmen, M.; Spevak, C. C.; Clutterbuck, J.; Kapitonov, V.; Jurka, J.; Scazzocchio, C.; Farman, M.; Butler, J.; Purcell, S.; Harris, S.; Braus, G. H.; Draht, O.; Busch, S.; D'Enfert, C.; Bouchier, C.; Goldman, G. H.; Bell-Pedersen, D.; Griffiths-Jones, S.; Doonan, J. H.; Yu, J.; Vienken, K.; Pain, A.; Freitag, M.; Selker, E. U.; Archer, D. B.; Peñalva, M. A.; Oakley, B. R.; Momany, M.; Tanaka, T.; Kumagai, T.; Asai, K.; Machida, M.; Nierman, W. C.; Denning, D. W.; Caddick, M.; Hynes, M.; Paoletti, M.; Fischer, R.; Miller, B.; Dyer, P.; Sachs, M. S.; Osmani, S. A.; Birren, B. W. Sequencing of *Aspergillus Nidulans* and Comparative Analysis with *A. Fumigatus* and *A. Oryzae*. *Nature* **2005**, *438*, 1105–1115.
- (37) Haldimann, A.; Prahald, M. K.; Fisher, S. L.; Kim, S.-K.; Walsh, C. T.; Wanner, B. L. Altered Recognition Mutants of the Response Regulator PhoB: A New Genetic Strategy for Studying Protein-Protein Interactions. *Proc. Natl. Acad. Sci. U.S.A.* **1996**, *93*, 14361–14366.
- (38) Schmitt, S.; Walser, M.; Rehmann, M.; Oesterle, S.; Panke, S.; Held, M. Archimedes' Principle for Characterisation of Recombinant Whole Cell Biocatalysts. *Sci. Rep.* **2018**, *8*, 3000.
- (39) Pautot, S.; Frisken, B. J.; Weitz, D. A. Engineering Asymmetric Vesicles. *Proc. Natl. Acad. Sci. U.S.A.* **2003**, *100*, 10718–10721.
- (40) Eyer, K.; Kuhn, P.; Hanke, C.; Dittrich, P. S. A Microchamber Array for Single Cell Isolation and Analysis of Intracellular Biomolecules. *Lab Chip* **2012**, *12*, 765–772.
- (41) Lin, C.-C.; Bachmann, M.; Bachler, S.; Venkatesan, K.; Dittrich, P. S. Tunable Membrane Potential Reconstituted in Giant Vesicles

Promotes Permeation of Cationic Peptides at Nanomolar Concentrations. *ACS Appl. Mater. Interfaces* **2018**, *10*, 41909–41916.

(42) Deshpande, S.; Dekker, C. On-Chip Microfluidic Production of Cell-Sized Liposomes. *Nat. Protoc.* **2018**, *13*, 856–874.

(43) Schindelin, J.; Arganda-Carreras, I.; Frise, E.; Kaynig, V.; Longair, M.; Pietzsch, T.; Preibisch, S.; Rueden, C.; Saalfeld, S.; Schmid, B.; Tinevez, J.-Y.; White, D. J.; Hartenstein, V.; Eliceiri, K.; Tomancak, P.; Cardona, A. Fiji: An Open-Source Platform for Biological-Image Analysis. *Nat. Methods* **2012**, *9*, 676–682.

(44) de Gier, J. Osmotic Behaviour and Permeability Properties of Liposomes. *Chem. Phys. Lipids* **1993**, *64*, 187–196.

(45) Chakrabarti, A. C. Permeability of Membranes to Amino Acids and Modified Amino Acids: Mechanisms Involved in Translocation. *Amino Acids* **1994**, *6*, 213–229.

(46) Deshpande, S.; Brandenburg, F.; Lau, A.; Last, M. G. F.; Spoelstra, W. K.; Reese, L.; Wunnava, S.; Dogterom, M.; Dekker, C. Spatiotemporal Control of Coacervate Formation within Liposomes. *Nat. Commun.* **2019**, *10*, 1800.